

Machine Learning-Based CSI Feedback With Variable Length in FDD Massive MIMO

Matteo Nerini, Valentina Rizzello, *Student Member, IEEE*, Michael Joham, *Member, IEEE*, Wolfgang Utschick, *Fellow, IEEE*, Bruno Clerckx, *Fellow, IEEE*

Abstract

To fully unlock the benefits of multiple-input multiple-output (MIMO) networks, downlink channel state information (CSI) is required at the base station (BS). In frequency division duplex (FDD) systems, the CSI is acquired through a feedback signal from the user equipment (UE). However, this may lead to an important overhead in FDD massive MIMO systems. Focusing on these systems, in this study, we propose a novel strategy to design the CSI feedback. Our strategy allows to optimally design the feedback with variable length, while reducing the parameter number at the UE. Specifically, principal component analysis (PCA) is used to compress the channel into a latent space with adaptive dimensionality. To quantize this compressed channel, the feedback bits are smartly allocated to the latent space dimensions by minimizing the normalized mean squared error (NMSE) distortion. Finally, the quantization codebook is determined with k -means clustering. Numerical simulations show that our strategy improves the zero-forcing beamforming sum rate by 26.8%, compared with the popular CsiNet. The number of model parameters is reduced by 24.9 times, thus causing a significantly smaller offloading overhead. At the same time, PCA is characterized by a lightweight unsupervised training, requiring eight times fewer training samples than CsiNet.

Index Terms

CSI Feedback, Massive MIMO, Frequency Division Duplex, Machine Learning, Principal Component Analysis, k -Means Clustering

M. Nerini and B. Clerckx are with the Department of Electrical and Electronic Engineering, Imperial College London, London, SW7 2AZ, U.K. (e-mail: {m.nerini20, b.clerckx}@imperial.ac.uk).

V. Rizzello, M. Joham and W. Utschick are with the Professur für Methoden der Signalverarbeitung, Technische Universität München, Munich, 80333, Germany. (e-mail: {valentina.rizzello, joham, utschick}@tum.de).

I. INTRODUCTION

Accurate knowledge of the wireless channel, or channel state information (CSI), is critical to unlock the full potential benefits of multiple-input multiple-output (MIMO) systems. In particular, CSI at the transmitter and at the receiver allow precoding and combining techniques, respectively, which can enhance the spectrum efficiency in MIMO wireless networks [1]. CSI at the transmitter can be easily acquired without feedback from the receiver in time division duplex (TDD) systems. In these systems, channel reciprocity holds since the uplink and downlink channels share the same frequency band. Conversely, CSI estimation at the transmitter is harder in frequency division duplex (FDD) systems, where the uplink-downlink channel reciprocity does not hold in general. Thus, feedback messages from the user equipment (UE) to the base station (BS) are needed to gain downlink CSI at the BS [2]. This may lead to significant overhead in massive MIMO systems, where a large number of antennas is employed. To face this problem, various strategies have been investigated, such as downlink training techniques [3], distributed compressive CSI estimation for multi-user settings [4], and adaptive CSI feedback depending on the channel sparsity [5]. Additionally, novel transmission strategies robust with respect to reduced-dimensional CSI have been proposed [6], [7], [8].

In recent years, deep learning (DL) techniques have been also used for CSI estimation in FDD systems, following two main research directions. In the first, the uplink-to-downlink channel mapping is learned. In this way, the feedback can be completely removed since the uplink channel knowledge at the BS is sufficient to gain also the downlink channel knowledge. In the second, the channel matrix is compressed with a DL architecture to minimize the feedback.

The uplink-to-downlink mapping existence was firstly investigated in [9]. In [9], [10], a fully connected neural network (NN) is used to map the uplink to the corresponding downlink channels. The same task is solved more efficiently in [11] with a sparse complex-valued NN, and in [12], [13] with a convolutional neural network (CNN) treating the space-frequency channel matrix as an image. Image processing techniques are exploited also in [14], [15]. In [14], the problem of inferring the downlink channel from the observed uplink is treated as an image completion problem, which is solved through a generative adversarial network (GAN). In [15], a convolutional and recurrent NN is proposed for predicting the downlink channel from the uplink considering also temporal variations. Finally, in [16], the channel is firstly compressed with an autoencoder to decrease the feature space dimensionality; then, the uplink-to-downlink mapping

is achieved with random forests. However, when more complex channel models are considered (e.g. accounting for a rich multipath and dynamic environment), the uplink-to-downlink mapping function becomes hard to approximate with NNs. The environment should be sampled with enough resolution to account for small-scale fading effects, which may require extensive sampling campaigns and huge datasets in practice. For this reason, the vast majority of related studies used DL techniques to reduce the feedback overhead, rather than completely remove it.

In [17], [18], a deep autoencoder is used to embed the downlink channel matrix at the UE into a latent space with reduced dimensionality. In this way, only the embedding of the channel matrix needs to be fed back to the BS. Deep autoencoder-like architectures have been proposed for the same scope in [19], [20], [21], [22], [23], [24]. The CsiNet architecture introduced in [19] is extended in [25] to exploit the temporal redundancy in a dynamic environment through recurrent layers, and further improved in [26]. In [20], the channel reconstruction accuracy is enhanced by exploiting also information from the uplink CSI, assumed available at the BS. In [21], a DL-based framework is proposed to jointly learn CSI compression and quantization. In [22], [23], [24], the CSI feedback is designed through lightweight DL architectures, characterized by a reduced number of trainable parameters. To improve the compression performance and reduce the model complexity, the novel concepts of network aggregation and layer binarization have been employed in [27]. Furthermore, the low rank structure of the millimeter wave channels has been exploited by the model-driven DL architecture proposed in [28].

Other related works employ DL techniques either at the BS or at the UE to improve the channel reconstruction quality or the feedback design, respectively. In [29], [30], the feedback is generated at the UE by sampling only specific entries of the downlink channel matrix. Then, the original channel matrix is reconstructed at the BS with image-restoration CNNs. Similarly, in [31], the channel is compressed at the UE based on compressive sensing and then recovered through a DL architecture at the BS. In [32], a NN has been proposed to directly map noisy pilot observations to their optimal feedback index. In this way, neither channel estimation nor knowledge of the feedback codebook are necessary at the UE. In [33], NNs are used to design an implicit CSI feedback mechanism in which the CSI is mapped into the recommended precoder. Finally, DL architectures have been applied to learn feedback messages with the objective of maximizing the downlink precoding performance in single-cell [34], and multi-cell [35] scenarios.

When applying DL models for designing the CSI feedback, three problems arise. First, very large training datasets are typically required: e.g., hundreds of thousands of downlink training

samples are used in many of the aforementioned studies [9], [11], [16], [17], [19], [23], [26], [27], [31], [33], [35]. This problem has been recently addressed by training the DL architectures solely with uplink channel samples, assumed available at the BS [30], [18], [32], [36]. These works exploit the conjecture that learning at the uplink frequency can be transferred at the downlink frequency with no further modification, as proposed for the first time in [30] and validated in [36]. Furthermore, this problem has been addressed through transfer learning in [37], where the authors investigate the trade-off between training cost and model performance. Second, deep autoencoders compress the channel into a latent space with fixed dimensionality, determined by the number of neurons present in their middle layer. As a result, when quantized feedback is considered, the latent space dimensionality cannot be adapted to the number of feedback bits. A solution to this problem is provided in [26], where the authors propose a DL-based method able to offer multiple compression ratios. However, the number of available compression ratios is still limited to a few units (e.g., four in [26]) due to the increasing number of trainable parameters at the decoder side. Third, each UE must encode the CSI by using the DL architecture trained at the BS. Thus, the trained architecture parameters need to be offloaded from the BS to the UE when a new UE connects to the BS, and after each training session (necessary to keep the DL model updated with the channel statistics). This causes an additional fixed overhead in the transmission, which cannot be reduced.

To solve these three problems typical of DL models, we propose a CSI compression strategy based on principal component analysis (PCA) [38]. Following [30], [36], our strategy avoids the use of downlink channel samples during the training session. In addition, our novel CSI compression strategy is characterized by a lightweight training phase for two reasons. Firstly, the number of training samples required is significantly reduced with respect to the aforementioned DL architectures. Secondly, PCA training does not involve iterative gradient-based optimization algorithms, which are computationally expensive. Differently from DL architectures, PCA allows to compress the channel into a latent space with adaptive dimensionality, depending on the number of principal components considered. It also allows to reduce the number of model parameters to be offloaded from the BS to the UE. The contributions of this paper are summarized as follows.

First, we propose a novel CSI feedback strategy based on PCA and k -means clustering. In this strategy, PCA is used to compress the channel matrix into a latent space with adaptive dimensionality, allowing to optimally design the feedback with variable length. To quantize this

compressed channel, the feedback bits are smartly allocated to the principal components in order to minimize a properly defined distortion function. Finally, on each principal component, the quantization levels are determined with k -means clustering.

Second, we provide theoretical justifications to prove the optimality of our bit allocation to the principal components. In particular, the bits are allocated to the principal components by minimizing the normalized mean squared error (NMSE) distortion introduced by the compression and quantization operations. A practical iterative algorithm is proposed to this scope, whose optimality is theoretically guaranteed.

Third, we propose an offloading overhead-aware CSI feedback strategy by improving our PCA-based strategy with two modifications. The first modification reduces the number of offloaded PCA parameters, while the second reduces the number of offloaded codebook parameters. With these two modifications, we introduce the possibility to adapt the number of offloaded parameters. Thus, the network operator can select the optimal trade-off between offloading overhead and channel reconstruction quality. To the best of our knowledge, an adaptive offloading overhead has never been considered in previous literature employing DL solutions. Numerical results show that these two modifications only slightly impact the reconstruction performance, while they significantly reduce the number of offloaded parameters.

Fourth, through numerical simulations, we compare the performance of our strategy with two state-of-the-art DL autoencoders proposed for the same scope. As a benchmark, we consider the popular CsiNet [19], and the autoencoder more recently proposed in [18] whose training is based on uplink data. Our strategy is characterized by a lightweight training phase, requiring significantly fewer training samples. The number of offloaded model parameters can be reduced with approximately no CSI reconstruction quality loss. Consequently, our strategy causes less offloading overhead than the considered reference autoencoders. At the same time, our strategy achieves better or approximately the same CSI reconstruction quality as these autoencoders.

It is worthwhile to remark the differences between our proposed CSI feedback strategy with previous works employing PCA for the same scope [39], [40]. First, we adapt the number of considered principal components according to the number of feedback bits available. When more feedback bits are available, more principal components can be considered for the compression, allowing an adaptive reconstruction quality. Second, we allocate the feedback bits to the latent space dimensions, i.e., the principal components, according to their importance. Third, to minimize the quantization error, we discretize the feedback by learning the optimal quantization

levels through k -means clustering. Fourth, we propose an overhead-aware strategy which aims at reducing the number of offloaded parameters from the BS to the UE.

Organization: In Section II, we define the system model and the problem formulation. In Section III, we present our novel CSI feedback strategy based on PCA and k -means clustering. In Section IV, we improve our CSI feedback strategy by proposing two modifications that allow to significantly decrease the number of parameters offloaded from the BS to the UEs. In Section V, we assess the obtained performance through numerical simulations. Finally, Section VI contains the concluding remarks.

Notation: Vectors and matrices are denoted with bold lower and bold upper letters, respectively. Scalars are represented with letters not in bold font. $|a|$, $\|\mathbf{a}\|$, and $\|\mathbf{A}\|_F$ refer to the absolute value of a complex scalar a , l_2 -norm of a vector \mathbf{a} , and Frobenius norm of a matrix \mathbf{A} , respectively. $[\mathbf{a}]_i$ denotes the i -th element of vector \mathbf{a} . \mathbf{A}^T and \mathbf{A}^H refer to the transpose and conjugate transpose of a matrix \mathbf{A} , respectively. \mathbb{N} , \mathbb{R} , and \mathbb{C} denote natural, real, and complex number sets, respectively. \mathbb{N}^* denotes the positive natural number set. $\mathbf{0}$ and \mathbf{I} refer to an all-zero matrix and an identity matrix, respectively. $\mathcal{CN}(0, \sigma^2)$ denotes the distribution of a circularly symmetric complex Gaussian (CSCG) random variable whose real and imaginary parts are independent normally distributed with mean zero and variance $\sigma^2/2$. $\mathcal{CN}(\mathbf{0}, \mathbf{R})$ denotes the distribution of a CSCG random vector with mean vector $\mathbf{0}$ and covariance matrix \mathbf{R} . Finally, $\text{diag}(a_1, \dots, a_N)$ refers to a diagonal matrix whose diagonal elements are a_1, \dots, a_N .

II. SYSTEM MODEL

Let us consider a multi-user MIMO system in which a BS equipped with N_A antennas serves K single-antenna users. Assuming an FDD communication system, we denote with f_{UL} and f_{DL} the uplink and downlink center frequencies, respectively. In both frequencies, the channel bandwidth W is divided into N_C orthogonal Frequency division multiplexing (OFDM) subcarriers.

We denote as $x_{\text{UL},q,n_C} \in \mathbb{C}$ the uplink signal transmitted by the q -th user on the n_C -th uplink subcarrier, and as $\mathbf{y}_{\text{UL},n_C} \in \mathbb{C}^{N_A \times 1}$ the uplink signal received by the BS on the n_C -th uplink subcarrier. Thus, we have

$$\mathbf{y}_{\text{UL},n_C} = \sum_{q=1}^K \mathbf{h}_{\text{UL},q,n_C} x_{\text{UL},q,n_C} + \mathbf{n}_{\text{UL},n_C}, \quad (1)$$

where $\mathbf{h}_{\text{UL},q,n_C} \in \mathbb{C}^{N_A \times 1}$ is the uplink channel vector seen by the q -th user on the n_C -th uplink subcarrier, and $\mathbf{n}_{\text{UL},n_C}$ is the additive white Gaussian noise (AWGN) at the n_C -th uplink

subcarrier. Similarly, we denote as $\mathbf{x}_{\text{DL},n_C} \in \mathbb{C}^{N_A \times 1}$ the downlink signal transmitted by the BS on the n_C -th downlink subcarrier, and as y_{DL,q,n_C} the downlink signal received by the q -th user on the n_C -th downlink subcarrier. Thus, we can write

$$y_{\text{DL},q,n_C} = \mathbf{h}_{\text{DL},q,n_C} \mathbf{x}_{\text{DL},n_C} + n_{\text{DL},q,n_C}, \quad (2)$$

where $\mathbf{h}_{\text{DL},q,n_C} \in \mathbb{C}^{1 \times N_A}$ is the downlink channel vector seen by the q -th user on the n_C -th downlink subcarrier, and n_{DL,q,n_C} is the AWGN at the n_C -th downlink subcarrier.

Let us define $\mathbf{H}_{\text{UL},q} = [\mathbf{h}_{\text{UL},q,1}, \mathbf{h}_{\text{UL},q,2}, \dots, \mathbf{h}_{\text{UL},q,N_C}] \in \mathbb{C}^{N_A \times N_C}$ as the uplink channel matrix and $\mathbf{H}_{\text{DL},q} = [\mathbf{h}_{\text{DL},q,1}^T, \mathbf{h}_{\text{DL},q,2}^T, \dots, \mathbf{h}_{\text{DL},q,N_C}^T] \in \mathbb{C}^{N_A \times N_C}$ as the downlink channel matrix of the q -th user. For simplicity of notation, we drop the index q in the rest of the paper. We assume that noisy versions of the uplink channel matrices are available at the BS, denoted as

$$\tilde{\mathbf{H}}_{\text{UL}} = \mathbf{H}_{\text{UL}} + \mathbf{N}_{\text{UL}}, \quad (3)$$

where the entries of $\mathbf{N}_{\text{UL}} \in \mathbb{C}^{N_A \times N_C}$ are CSCG distributed such that $\mathbb{E}[\|\mathbf{H}_{\text{UL}}\|_F^2 / \|\mathbf{N}_{\text{UL}}\|_F^2] = \text{SNR}_{\text{UL}}$. Similarly, a noisy version of the downlink channel matrix is available at each UE, which is given by

$$\tilde{\mathbf{H}}_{\text{DL}} = \mathbf{H}_{\text{DL}} + \mathbf{N}_{\text{DL}}, \quad (4)$$

where $\mathbb{E}[\|\mathbf{H}_{\text{DL}}\|_F^2 / \|\mathbf{N}_{\text{DL}}\|_F^2] = \text{SNR}_{\text{DL}}$. In this system model, our goal is to reconstruct the downlink CSI \mathbf{H}_{DL} at the BS from limited feedback sent by the UE. To this end, we compress and quantize the CSI using two machine learning (ML) techniques: PCA and k -means clustering.

III. PCA AND k -MEANS CLUSTERING-BASED CSI FEEDBACK DESIGN

In this section, we describe our novel channel estimation process, which consists of two stages. In the first stage, called *offline learning*, the compression strategy is learned at the BS, based on a reduced training dataset. This stage has three objectives: learning the principal components to compress the CSI, allocating the feedback bits to the first principal components, and learning the quantization levels through k -means clustering. In the second stage, called *online development*, the CSI is compressed and quantized at the UE, sent to the BS, and here reconstructed, as graphically represented in Fig. 1.

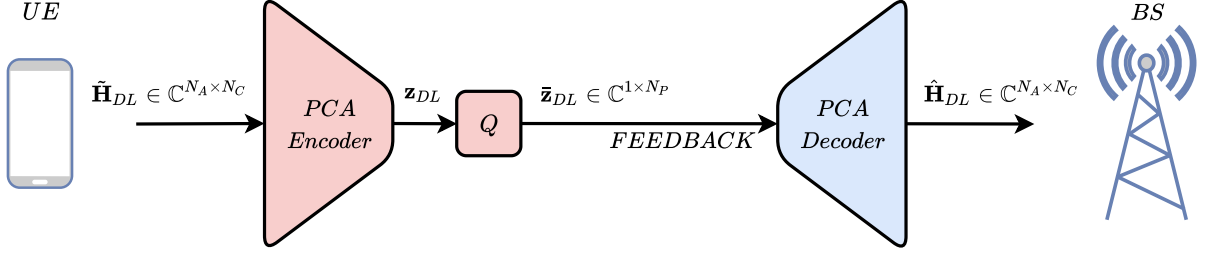


Fig. 1. Downlink channel estimation at the BS with quantized feedback from the UE.

A. Offline Learning

To learn the principal components, we propose an offline training stage carried out at the BS. To this end, we consider a training set solely composed of noisy uplink channels, assumed available at the BS. This approach is based on the conjecture that learning at the uplink frequency can be transferred at the downlink frequency with no further modification [30], [36]. In this way, downlink CSI samples, which are hard to collect at the BS, are not required in the training stage. Let us denote with N_{train} the number of training samples, and with $\tilde{\mathbf{H}}_{\text{train}} \in \mathbb{C}^{N_{\text{train}} \times N_A N_C}$ the training set, whose rows are vectorized noisy uplink channels. Furthermore, we denote with $\boldsymbol{\mu}_{\text{train}}$ the column-wise mean of $\tilde{\mathbf{H}}_{\text{train}}$, and with $\mathbf{H}_{\text{train}}$ the centered training set obtained by subtracting $\boldsymbol{\mu}_{\text{train}}$ to each row of $\tilde{\mathbf{H}}_{\text{train}}$. Thus, the sample covariance matrix of the training set can be obtained as

$$\mathbf{R} = \frac{\mathbf{H}_{\text{train}}^H \mathbf{H}_{\text{train}}}{N_{\text{train}} - 1}. \quad (5)$$

With eigenvalue decomposition, \mathbf{R} can be factorized as $\mathbf{R} = \mathbf{V} \boldsymbol{\Lambda} \mathbf{V}^H$, where \mathbf{V} is a unitary matrix whose columns are the principal components, and $\boldsymbol{\Lambda} = \text{diag}(\sigma_1^2, \dots, \sigma_{N_A N_C}^2)$ is a diagonal matrix containing the $N_A N_C$ eigenvalues. Let us assume that the eigenvalues in $\boldsymbol{\Lambda}$ have been sorted in descending order, and that their respective eigenvectors in \mathbf{V} (i.e., the principal components) have been ordered accordingly. Thus, we can select the conversion matrix $\mathbf{V}_{N_P} \in \mathbb{C}^{N_A N_C \times N_P}$, containing the first N_P columns of \mathbf{V} , to project the data onto a latent space with dimensionality N_P .

After the dimensionality reduction operation, the compressed CSI needs to be discretized and represented with a limited number of bits B . According to a naive discretization approach, we could fix the latent space dimensionality N_P arbitrarily, and quantize the compressed CSI by allocating B/N_P bits to each principal component. However, this approach would be suboptimal

for two reasons. Firstly, N_P should be defined according to the number of feedback bits B . A higher B should allow a larger latent space dimensionality N_P , while, vice versa, a lower B should reduce N_P . Secondly, the N_P principal components have decreasing importance, defined as the variance explained by each of them. Thus, the optimal discretization approach is expected to allocate more bits to more important principal components, and fewer bits to the less important ones. To solve these two problems, we propose to allocate the B bits to the principal components in a way that minimizes the distortion introduced by the compression and quantization operations. As a result of this bit allocation process, the number of bits allocated to each principal component is described by the vector $\mathbf{b} = [b_1, \dots, b_{N_A N_C}] \in \mathbb{N}^{N_A N_C}$, where b_n is the number of bits allocated to the n -th principal component. Thus, we have $\sum_{n=1}^{N_A N_C} b_n = B$ and N_P is given by the index of the last non-zero element in \mathbf{b} . The proposed bit allocation process is described in detail in Subsection III-C.

After determining N_P and the bit allocation to the first N_P principal components, the quantization levels need to be specified. To minimize the quantization distortion, measured in terms of mean squared error (MSE), we define different quantization levels for each principal component, based on k -means clustering [38]. To this end, we project the training set $\mathbf{H}_{\text{train}}$ onto the first N_P principal components, obtaining $\mathbf{Z}_{\text{train}} = \mathbf{H}_{\text{train}} \mathbf{V}_{N_P} \in \mathbb{C}^{N_{\text{train}} \times N_P}$. In this way, the rows of $\mathbf{Z}_{\text{train}}$ are the embeddings of the training set elements into the latent space. Then, k -means clustering is applied independently to each column of $\mathbf{Z}_{\text{train}}$, where for the n -th column we have $k = 2^{b_n}$. Since each column of $\mathbf{Z}_{\text{train}}$ is a complex vector, each k -means clustering problem is considered as a vector quantization problem in the feature space \mathbb{R}^2 . In this problem, the two dimensions are given by the real and imaginary parts of the $\mathbf{Z}_{\text{train}}$ elements. Finally, the cluster centers of the n -th k -means clustering give the quantization levels for the n -th latent space dimension.

B. Online Development

After the *offline learning* stage, the first N_P principal components, the vector $\boldsymbol{\mu}_{\text{train}}$, and the codebook of the learned quantization levels are offloaded to the UE. This allows the online feedback process, as represented in Fig. 1. The UE firstly vectorizes the noisy downlink channel matrix $\tilde{\mathbf{H}}_{\text{DL}}$ into $\tilde{\mathbf{h}}_{\text{DL}} \in \mathbb{C}^{1 \times N_A N_C}$. Then, it compresses $\mathbf{h}_{\text{DL}} = \tilde{\mathbf{h}}_{\text{DL}} - \boldsymbol{\mu}_{\text{train}}$ by considering only the first N_P principal components, obtaining $\mathbf{z}_{\text{DL}} = \mathbf{h}_{\text{DL}} \mathbf{V}_{N_P} \in \mathbb{C}^{1 \times N_P}$. Before the feedback transmission, the compressed CSI \mathbf{z}_{DL} is quantized according to the learned codebook. Therefore, $\bar{\mathbf{z}}_{\text{DL}}$ is obtained by mapping the \mathbf{z}_{DL} entries to their nearest cluster centers. In this way, the

feedback is fully described by B bits, which are sent from the UE to the BS. Finally, the downlink channel estimation process is concluded at the BS. Here, the decoder firstly calculates $\hat{\mathbf{h}}_{\text{DL}} = \bar{\mathbf{z}}_{\text{DL}} \mathbf{V}_{N_P}^H \in \mathbb{C}^{1 \times N_A N_C}$; and secondly, it reshapes $\hat{\mathbf{h}}_{\text{DL}} + \boldsymbol{\mu}_{\text{train}}$ into $\hat{\mathbf{H}}_{\text{DL}}$, which is the downlink channel matrix estimate.

C. Bit Allocation to the Principal Components

Within the the *offline learning* stage, the optimal bit allocation to the principal components is learned. As anticipated, this is achieved by minimizing the distortion introduced by the compression and quantization operations. To measure such a distortion, we define a distortion function D_f given by the NMSE between the reconstructed vectorized channel $\hat{\mathbf{h}}_{\text{DL}}$ and the actual vectorized channel available at the UE \mathbf{h}_{DL}

$$D_f = \mathbb{E} \left[\frac{\|\mathbf{h}_{\text{DL}} - \hat{\mathbf{h}}_{\text{DL}}\|^2}{\|\mathbf{h}_{\text{DL}}\|^2} \right], \quad (6)$$

where the average is over all the channel realizations in the training set. Without loss of generality, we can write $\mathbf{h}_{\text{DL}} = \mathbf{g}_{\text{DL}} \mathbf{V}^H$, where $\mathbf{g}_{\text{DL}} = \mathbf{h}_{\text{DL}} \mathbf{V}$ is the mapping of \mathbf{h}_{DL} into the entire principal component space, and $\hat{\mathbf{h}}_{\text{DL}} = \bar{\mathbf{g}}_{\text{DL}} \mathbf{V}^H$, where $\bar{\mathbf{g}}_{\text{DL}}$ is the quantized version of \mathbf{g}_{DL} . Thus, the distortion function D_f can be rewritten as

$$D_f = \mathbb{E} \left[\frac{\|\mathbf{g}_{\text{DL}} \mathbf{V}^H - \bar{\mathbf{g}}_{\text{DL}} \mathbf{V}^H\|^2}{\|\mathbf{h}_{\text{DL}}\|^2} \right] \quad (7)$$

$$= \mathbb{E} \left[\frac{\|(\mathbf{g}_{\text{DL}} - \bar{\mathbf{g}}_{\text{DL}}) \mathbf{V}^H\|^2}{\|\mathbf{h}_{\text{DL}}\|^2} \right] \quad (8)$$

$$\leq \mathbb{E} \left[\frac{\|\mathbf{g}_{\text{DL}} - \bar{\mathbf{g}}_{\text{DL}}\|^2 \|\mathbf{V}^H\|_F^2}{\|\mathbf{h}_{\text{DL}}\|^2} \right] = \bar{D}_f, \quad (9)$$

where the inequality follows from the Cauchy-Schwarz inequality. We now assume that the training set has been normalized such that for every channel we have $\|\mathbf{h}_{\text{DL}}\|^2 = N_A N_C$. This has no impact on the multi-user precoding performance since the precoder design only requires the channel direction information (CDI). Thus, noting that $\|\mathbf{V}^H\|_F^2$ and $\|\mathbf{h}_{\text{DL}}\|^2$ are constant, the

upper bound on the distortion function \bar{D}_f can be simplified as

$$\bar{D}_f = \mathbb{E} [\|\mathbf{g}_{\text{DL}} - \bar{\mathbf{g}}_{\text{DL}}\|^2] \quad (10)$$

$$= \mathbb{E} \left[\sum_{n=1}^{N_A N_C} |[\mathbf{g}_{\text{DL}}]_n - [\bar{\mathbf{g}}_{\text{DL}}]_n|^2 \right] \quad (11)$$

$$= \sum_{n=1}^{N_A N_C} \mathbb{E} [|[\mathbf{g}_{\text{DL}}]_n - [\bar{\mathbf{g}}_{\text{DL}}]_n|^2]. \quad (12)$$

We notice that the term $\mathbb{E} [|[\mathbf{g}_{\text{DL}}]_n - [\bar{\mathbf{g}}_{\text{DL}}]_n|^2]$ is the MSE due to the quantization of the n -th principal component. The MSE is a common metric used to measure the distortion in lossy compression. Thus, to simplify the notation, we introduce the vector $\mathbf{d} = [d_1, \dots, d_{N_A N_C}]$, where $d_n = \mathbb{E} [|[\mathbf{g}_{\text{DL}}]_n - [\bar{\mathbf{g}}_{\text{DL}}]_n|^2]$. Consequently, our objective becomes to find the bit allocation \mathbf{b} such that $\bar{D}_f = \sum_{n=1}^{N_A N_C} d_n$ is minimized. Here, the implicit dependence of \bar{D}_f on \mathbf{b} lies in the fact that the distortion d_n depends on the number of bits b_n used to quantize the n -th principal component, and on the quantization strategy employed. Since the fixed-rate quantization strategy that minimizes d_n is k -means clustering, we consider d_n as the minimum distortion obtainable by k -means clustering with $k = 2^{b_n}$. In the following, we write $d_n = d_n(b_n)$ to highlight that d_n is a function purely dependent on b_n .

To design an algorithm able to find the optimal bit allocation \mathbf{b} , we now introduce two useful propositions. Let us assume that the channels are Rayleigh distributed, with covariance matrix \mathbf{R} . Thus, we have that the rows of $\mathbf{H}_{\text{train}}$ are distributed as $\mathcal{CN}(\mathbf{0}, \mathbf{R})$. Recalling that $\mathbf{R} = \mathbf{V}\mathbf{\Lambda}\mathbf{V}^H$, the rows of $\mathbf{G}_{\text{train}} = \mathbf{H}_{\text{train}}\mathbf{V}$ are distributed as $\mathcal{CN}(\mathbf{0}, \mathbf{\Lambda})$ [41]. In other words, since $\mathbf{G}_{\text{train}}$ is the training set projection onto the whole principal components space, we obtain that on every principal component the training set entries are CSCG distributed. More precisely, each entry of the n -th column of $\mathbf{G}_{\text{train}}$ is distributed as $\mathcal{CN}(0, \sigma_n^2)$, meaning that on the n -th principal component the training set entries are distributed as $\mathcal{CN}(0, \sigma_n^2)$. This property is used to derive the following two propositions.

Proposition 1. *If the optimal allocation of B bits is $\mathbf{b} = [b_1, \dots, b_{N_A N_C}]$, the optimal allocation of $B + 1$ bits is $\mathbf{b}' = [b_1, \dots, b_m + 1, \dots, b_{N_A N_C}]$ for some index $m \in [1, N_A N_C]$.*

Proof. Please refer to Appendix A. □

In other words, the optimal allocation of $B + 1$ bits can be obtained from the optimal allocation

Algorithm 1: Bit allocation to the principal components.

Input: $B, \mathbf{G}_{\text{train}}$
Output: \mathbf{b}

```

1  $\mathbf{b} \leftarrow [0, \dots, 0] \in \mathbb{N}^{N_A N_C};$ 
2 for  $i \leftarrow 1$  to  $B$  do
3    $\Delta \mathbf{d} \leftarrow [0, \dots, 0] \in \mathbb{R}^{N_A N_C};$ 
4   for  $n \leftarrow 1$  to  $N_A N_C$  do
5     if  $n == 1$  then
6        $\Delta d_n \leftarrow d_n(b_n) - d_n(b_n + 1);$ 
7     else if  $b_n < b_{n-1}$  then
8        $\Delta d_n \leftarrow d_n(b_n) - d_n(b_n + 1);$ 
9     end
10  end
11   $[\sim, m] \leftarrow \max(\Delta \mathbf{d});$ 
12   $b_m \leftarrow b_m + 1;$ 
13 end
14 return  $\mathbf{b}$ 

```

of B bits by adding one bit to the m -th principal component, for some $m \in [1, N_A N_C]$. This allows us to recursively find the optimal bit allocation.

Proposition 2. *If the optimal allocation of B bits is $\mathbf{b} = [b_1, \dots, b_{N_A N_C}]$, we have $b_n \leq b_{n-1} \forall n \in [2, N_A N_C]$.*

Proof. Please refer to Appendix B. □

Note that the \mathbf{b} elements are non increasing since the principal components are ordered according to their importance. This agrees with our intuition that more feedback bits should be allocated to more important principal components, and fewer bits to the less important ones.

We now use these two propositions to find the optimal bit allocation \mathbf{b} through Algorithm 1. The objective of Algorithm 1 is to return the bit allocation vector \mathbf{b} that minimizes the distortion function $\bar{D}_f = \sum_{n=1}^{N_A N_C} d_n$. To do so, we propose an iterative approach in which one bit at a time is added in \mathbf{b} , until all B bits are allocated, i.e., until $\sum_{n=1}^{N_A N_C} b_n = B$. Note that this iterative approach is able to lead to the optimal bit allocation because of Proposition 1. At the i -th iteration, the index of the \mathbf{b} element receiving the i -th bit could be found with exhaustive search. More precisely, for all the $N_A N_C$ principal components, the decrease in distortion caused by the

additional bit could be computed and stored in the vector $\Delta \mathbf{d} = [\Delta d_1, \dots, \Delta d_{N_A N_C}] \in \mathbb{R}^{N_A N_C}$, where $\Delta d_n = d_n(b_n) - d_n(b_n + 1)$. Consequently, the i -th bit could be allocated to the principal component experiencing the highest decrease in distortion (i.e., the m -th principal component in Algorithm 1). However, this exhaustive search would require to explore $N_A N_C$ possibilities for the allocation of each bit. To significantly reduce the search space from $N_A N_C$ to only a few plausible principal components we resort to Proposition 2. If at the i -th iteration we have $b_n = b_{n-1}$, the n -th principal component will certainly not receive the i -th bit. Thus, the index n can be excluded from the search. As a consequence of Proposition 2, the number of plausible principal components that are eligible to receive the i -th bit becomes $b_1 + 1$ (i.e., a few units in practice).

The inputs of Algorithm 1 are the number of feedback bits B , and the matrix $\mathbf{G}_{\text{train}}$, representing the projection of the training set $\mathbf{H}_{\text{train}}$ onto the whole principal components space. Here, $\mathbf{G}_{\text{train}}$ is needed to compute $d_n(b_n)$ through k -means clustering.¹ Furthermore, $d_n(0)$ is the maximum distortion for the n -th principal component, obtained by quantizing it with 0 bits. Thus, we have that $d_n(0)$ is the variance of the n -th column of $\mathbf{G}_{\text{train}}$, i.e., $d_n(0) = \sigma_n^2$. Finally, the output of Algorithm 1 is the vector \mathbf{b} , whose n -th element represents the number of bits allocated to the n -th principal component. The latent space dimensionality N_P is returned implicitly as the index of the last non-zero element in \mathbf{b} .

Let us remark that this bit allocation strategy is possible because of a specific property of PCA. In PCA, once the matrix \mathbf{V} is constructed upon a single training phase, all the latent space dimensionalities $N_P \in [1, \min\{N_{\text{train}} - 1, N_A N_C\}]$ can be considered for compression. Conversely, in a deep autoencoder, this degree of freedom is not present since the latent space dimensionality is completely determined by the number of its middle layer neurons.

IV. OFFLOADING OVERHEAD-AWARE CSI FEEDBACK DESIGN

When using a DL-based or PCA-based CSI feedback strategy, the relevant model parameters need to be offloaded from the BS to the UE after the training phase. In the case of DL-based CSI feedback, these parameters are the weights of the neurons composing the deep architecture involved. In the case of PCA-based CSI feedback, these parameters are the element of the complex matrix \mathbf{V}_{N_P} and the complex vector $\boldsymbol{\mu}_{\text{train}}$. Additionally, in both cases, the actual

¹Note that if $N_{\text{train}} \leq N_A N_C$, only the first $N_{\text{train}} - 1$ columns of $\mathbf{G}_{\text{train}}$ are not null. Nevertheless, this does not affect our discussion if N_{train} is sufficiently large, i.e., $N_{\text{train}} > N_P$, where N_P is the last non-zero element in \mathbf{b} .

feedback is a quantized version of the compressed channel. When k -means clustering is used to minimize the MSE, also the optimal quantization levels need to be offloaded from the BS to the UE. This necessary offloading process causes an additional overhead in the transmission. Thus, it is crucial to design a CSI feedback strategy being aware that this overhead should be minimum. In this section, we propose two modifications to our PCA-based CSI feedback strategy to reduce the number of offloaded variables. The first modification reduces the number of offloaded PCA parameters, while the second reduces the number of offloaded k -means clustering levels.

A. Reduction of the Number of Offloaded Model Parameters

In our PCA-based CSI feedback as proposed in Section III, the UE needs \mathbf{V}_{N_P} in order to compress the channel along the first N_P principal components. Thus, the number of real model parameters which are offloaded is

$$N_O^{\text{model}} = 2N_A N_C N_P + 2N_A N_C, \quad (13)$$

where the two additive terms are respectively due to the complex matrix \mathbf{V}_{N_P} and the complex vector $\boldsymbol{\mu}_{\text{train}}$. To decrease this number, we observe that the principal components can be sparsified in the angular-delay domain. Let us now consider the general case in which the BS is a uniform planar array (UPA) with dimensions $N_X \times N_Y$, where $N_X N_Y = N_A$. Here, we define $\mathbf{v}_n \in \mathbb{C}^{N_A N_C \times 1}$ as the n -th principal component, i.e., the n -th column of \mathbf{V}_{N_P} . This vector \mathbf{v}_n can be reshaped into a tensor of dimensions $N_X \times N_Y \times N_C$ in order to highlight its two spatial and frequency domains. We denote the vectorized 3-dimensional discrete Fourier transform (DFT3) of such a tensor as $\mathbf{f}_n \in \mathbb{C}^{N_A N_C \times 1}$. Thus, \mathbf{f}_n turns out to be sparse since it contains the information of \mathbf{v}_n in the two angular and delay domains. In this way, each principal component \mathbf{v}_n can be approximately reconstructed by considering only the significantly non-zero entries of \mathbf{f}_n .

To decrease the number of offloaded model parameters by exploiting this sparsity property, we introduce a new design parameter η , such that only a fraction $1/\eta$ of all the \mathbf{f}_n entries is offloaded, with $\eta \in [1, N_A N_C]$. In detail, let us define the binary mask vector $\mathbf{m}_n \in \{0, 1\}^{N_A N_C \times 1}$, containing $\frac{N_A N_C}{\eta}$ ones in correspondence of the largest values in \mathbf{f}_n .² To retain only the most significant $\frac{N_A N_C}{\eta}$ values from \mathbf{f}_n , we consider the Hadamard product $\tilde{\mathbf{f}}_n = \mathbf{f}_n \odot \mathbf{m}_n$. Thus, the sparse vector $\tilde{\mathbf{f}}_n$ is offloaded from the BS to the UE instead of \mathbf{v}_n . In matrix form, we have

²The wording “largest” is intended in terms of absolute value, since the \mathbf{f}_n elements are complex.

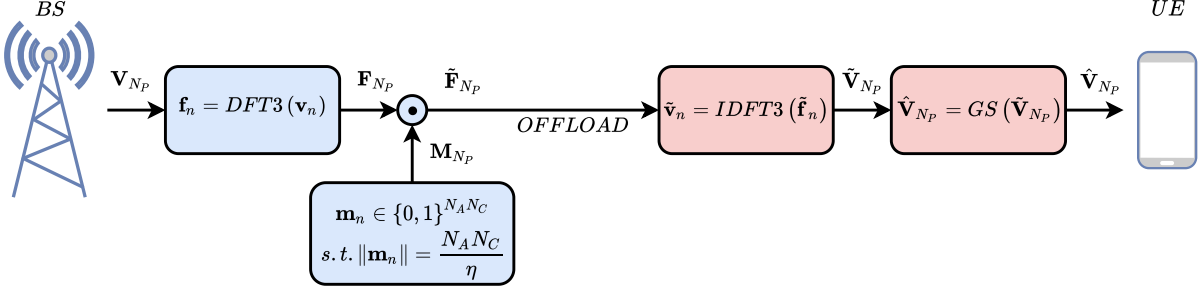


Fig. 2. Model parameters offload from the BS to the UE.

that $\tilde{\mathbf{F}}_{N_P} = \mathbf{F}_{N_P} \odot \mathbf{M}_{N_P}$ is offloaded instead of \mathbf{V}_{N_P} , where $\tilde{\mathbf{F}}_{N_P} = [\tilde{\mathbf{f}}_1, \dots, \tilde{\mathbf{f}}_{N_P}]$, $\mathbf{F}_{N_P} = [\mathbf{f}_1, \dots, \mathbf{f}_{N_P}]$, and $\mathbf{M}_{N_P} = [\mathbf{m}_1, \dots, \mathbf{m}_{N_P}]$.

At the UE side, each vector $\tilde{\mathbf{f}}_n$ is firstly reshaped into a tensor of dimensions $N_X \times N_Y \times N_C$. Then, each principal component $\tilde{\mathbf{v}}_n$ is obtained by vectorizing the 3-dimensional inverse discrete Fourier transform (IDFT3) of such a tensor. Note that the resulting matrix $\tilde{\mathbf{V}}_{N_P} = [\tilde{\mathbf{v}}_1, \dots, \tilde{\mathbf{v}}_{N_P}]$ is nearly semi-unitary, i.e., $\tilde{\mathbf{V}}_{N_P}^H \tilde{\mathbf{V}}_{N_P} \approx \mathbf{I}$, but not semi-unitary since the least significant entries in \mathbf{F}_{N_P} have been pruned to reduce the offloading overhead. For this reason, a last step is needed to ensure that the reconstructed principal component matrix $\hat{\mathbf{V}}_{N_P} = [\hat{\mathbf{v}}_1, \dots, \hat{\mathbf{v}}_{N_P}]$ is semi-unitary, i.e., $\hat{\mathbf{v}}_n \perp \hat{\mathbf{v}}_m \forall n \neq m$ and $\|\hat{\mathbf{v}}_n\| = 1 \forall n$. This is achieved by applying the Gram-Schmidt process to the columns of $\tilde{\mathbf{V}}_{N_P}$ yielding $\hat{\mathbf{V}}_{N_P} = \text{GS}(\tilde{\mathbf{V}}_{N_P})$.³ To summarize, the proposed modification to reduce the number of offloaded model parameters is graphically represented in Fig. 2.

The channel embedding \mathbf{z}_{DL} is now computed at the UE using $\hat{\mathbf{V}}_{N_P}$ instead of the exact matrix \mathbf{V}_{N_P} . Thus, the optimal bit allocation and the quantization levels should also be computed at the BS using the training set projection onto $\hat{\mathbf{V}} = [\hat{\mathbf{v}}_1, \dots, \hat{\mathbf{v}}_{N_A N_C}]$. To this end, all the aforementioned operations are applied at the BS as part of the offline training process. More precisely, after the matrix \mathbf{V} is computed with PCA, it is directly transformed into $\hat{\mathbf{V}}$ by applying the aforementioned operations. The only difference with the process depicted in Fig. 2 is that in this case the operations are not limited to the first N_P principal components. Subsequently,

³This Gram-Schmidt process has complexity $\mathcal{O}(N_A N_C N_P^2)$. Since it is needed only during the offline training stage, we assume that it can be performed at the UE with a negligible impact on the energy consumption. Alternatively, this operation can be replaced by computing the orthogonal factor of the polar decomposition of $\tilde{\mathbf{V}}_{N_P}$ as $\hat{\mathbf{V}}_{N_P} = \tilde{\mathbf{V}}_{N_P} (\tilde{\mathbf{V}}_{N_P}^H \tilde{\mathbf{V}}_{N_P})^{-1/2}$, or its first order Taylor approximation as $\hat{\mathbf{V}}_{N_P} = \tilde{\mathbf{V}}_{N_P} - \frac{1}{2} \tilde{\mathbf{V}}_{N_P} (\tilde{\mathbf{V}}_{N_P}^H \tilde{\mathbf{V}}_{N_P} - \mathbf{I})$. Gram-Schmidt has been selected since it has the lowest complexity and the best reconstruction accuracy among the three.

$\hat{\mathbf{G}}_{\text{train}} = \mathbf{H}_{\text{train}} \hat{\mathbf{V}}$ is used in Algorithm 1 instead of $\mathbf{G}_{\text{train}}$ to compute the optimal bit allocation and N_P . In addition, $\hat{\mathbf{Z}}_{\text{train}} = \mathbf{H}_{\text{train}} \hat{\mathbf{V}}_{N_P}$ is used to find the optimal quantization levels with k -means clustering instead of $\mathbf{Z}_{\text{train}}$.

With this modification, the number of offloaded real model parameters is reduced to

$$N_O^{\text{model}} = 2 \frac{N_A N_C}{\eta} N_P + \frac{N_A N_C}{\eta} N_P + 2 N_A N_C, \quad (14)$$

where the three additive terms are respectively due to the non-zero complex elements of $\tilde{\mathbf{F}}_{N_P}$, the positions of these elements within $\tilde{\mathbf{F}}_{N_P}$, and the complex vector $\boldsymbol{\mu}_{\text{train}}$. Finally, we remark that this modification allows to introduce an adaptive offloading overhead, as a function of η . Thus, η could be designed by the network operator as an adaptive parameter to trade offloading overhead impact with channel reconstruction quality. This degree of freedom is not present in the existing literature where DL architectures are used for CSI feedback.

B. Reduction of the Number of Offloaded k -means Clustering Parameters

Let us now assume that the bit allocation $\mathbf{b} = [b_1, \dots, b_{N_A N_C}]$ and N_P have been designed through Algorithm 1 considering B as the maximum feedback length allowed. In our PCA-based CSI feedback as proposed in Section III, the quantization levels are obtained for each principal component, generating N_P codebooks which all need to be offloaded from the BS to the UE. Thus, to allow the UE to generate a feedback of any length less or equal than B , we need to offload a codebook including $\sum_{r=1}^{b_n} 2^r$ complex quantization levels for the n -th principal component. In addition, for any feedback length less or equal than B , the UE needs to know the bit allocation, i.e., how the bits are allocated to the principal components. To provide the UE with all the possible bit allocations, the BS offloads the vector $\mathbf{m} = [m_1, \dots, m_B]$, where m_i is the index of the principal component receiving the i -th bit in Algorithm 1. The vector \mathbf{m} is sufficient to describe all the bit allocations with length from 1 to B because of Proposition 1. Eventually, the number of real k -means clustering parameters which are offloaded is

$$N_O^{k\text{-means}} = \left(2 \sum_{n=1}^{N_P} \sum_{r=1}^{b_n} 2^r \right) + B, \quad (15)$$

where the two additive terms are respectively due to the complex k -means clustering levels and the vector \mathbf{m} .

Now, our goal is to decrease the number of offloaded k -means clustering levels by considering a unique codebook that can be automatically adapted at the UE to fit all the N_P principal components. To this end, we exploit the fact that when a dataset is scaled, also its optimal k -means clustering quantization levels experience the same scaling, as formalized in the following proposition.

Proposition 3. *Let us consider a generic dataset $\mathbf{X} \in \mathbb{R}^{N \times D}$ containing N D -dimensional points, and a real scalar $c > 0$. If the optimal k -means clustering quantization levels of \mathbf{X} are $\{\mathbf{q}_i\}^*$, the optimal k -means clustering quantization levels of the dataset $\mathbf{Y} = c\mathbf{X}$ are $\{\mathbf{q}'_i\}^* = c\{\mathbf{q}_i\}^*$.*

Proof. Please refer to Appendix C. □

Such a unique codebook is constructed by introducing the matrix $\check{\mathbf{Z}}_{\text{train}}$, obtained by column-wise dividing $\hat{\mathbf{Z}}_{\text{train}}$ by the vector $\boldsymbol{\sigma} = [\sigma_1, \dots, \sigma_{N_P}]$. In other words, all the columns in $\hat{\mathbf{Z}}_{\text{train}}$ have been normalized in $\check{\mathbf{Z}}_{\text{train}}$ such that they have unitary variance. Thus, we can now design a codebook which is optimal for all the columns in $\check{\mathbf{Z}}_{\text{train}}$, assuming that their elements are identically distributed. To do so, we vectorize the matrix $\check{\mathbf{Z}}_{\text{train}}$ into the vector $\check{\mathbf{z}}_{\text{train}}$, and we apply k -means clustering to $\check{\mathbf{z}}_{\text{train}}$ considering $k = 2^r$ with $r \in [1, b_1]$, where b_1 is the first element of \mathbf{b} . We denote the quantization levels of the resulting codebook as $\{\mathbf{q}_i\}^*$. Finally, according to Proposition 3, we obtain the quantization levels for the n -th column of $\hat{\mathbf{Z}}_{\text{train}}$ (i.e., for the n -th principal component) by simply computing $\sigma_n\{\mathbf{q}_i\}^*$.

With this modification, the number of real k -means clustering parameters which are offloaded is given by

$$N_O^{k\text{-means}} = \left(2 \sum_{r=1}^{b_1} 2^r \right) + N_P + B, \quad (16)$$

where the three additive terms are respectively due to the codebook containing the complex quantization levels, the vector $\boldsymbol{\sigma}$ used to adapt the codebook to each principal component, and the vector \mathbf{m} used to obtain the bit allocation.

We finally remark that the number of offloaded parameters considered in this section is to be intended per user. Nevertheless, in multi-user scenarios, this information is common to all the users connected to the BS. Thus, the model parameters and the k -means clustering levels can be broadcasted to all the intended users in these scenarios, without further increasing the offloading overhead.

V. NUMERICAL RESULTS

In this section, we provide numerical results to evaluate our proposed CSI feedback strategy, and compare it with state-of-the-art DL architectures proposed for the same scope. The performance is measured in terms of downlink channel reconstruction quality, assessed by considering three metrics:

- the NMSE between the estimated downlink channel $\hat{\mathbf{H}}_{\text{DL}}$ and the true downlink channel \mathbf{H}_{DL} , defined as

$$NMSE = \frac{\|\hat{\mathbf{H}}_{\text{DL}} - \mathbf{H}_{\text{DL}}\|_F^2}{\|\mathbf{H}_{\text{DL}}\|_F^2}; \quad (17)$$

- the cosine similarity between $\hat{\mathbf{H}}_{\text{DL}}$ and \mathbf{H}_{DL} , defined as

$$\rho = \frac{1}{N_C} \sum_{n_C=1}^{N_C} \frac{|\hat{\mathbf{h}}_{n_C}^H \mathbf{h}_{n_C}|}{\|\hat{\mathbf{h}}_{n_C}\| \|\mathbf{h}_{n_C}\|}, \quad (18)$$

where $\hat{\mathbf{h}}_{n_C}$ and \mathbf{h}_{n_C} are the n_C -th columns of $\hat{\mathbf{H}}_{\text{DL}}$ and \mathbf{H}_{DL} , respectively;

- the average sum rate obtained with zero-forcing beamforming and water-filling power allocation.

In addition, we assess the considered CSI feedback strategies in terms of offloading overhead (i.e., the number of offloaded model parameters) and in terms of number of training samples required.

A. Dataset Description

The channels for both training and test sets were generated with QuaDRiGa version 2.4, a MATLAB based statistical ray-tracing channel simulator [42]. To this end, we consider an urban microcell in which single-antenna UEs are uniformly distributed at a distance included in the interval $[20, 100]$ m from the BS, and at a height of 1.5 m over the ground. The links between the BS and the UEs are non-line-of-sight (NLoS), and $L = 58$ paths are considered to simulate a rich multipath environment. The BS, 20 m high, is a UPA composed of $N_A = 64$ antennas. These array elements are arranged on an $N_X \times N_Y$ shape with an antenna spacing of half wavelength, where $N_X = 8$ and $N_Y = 8$. The uplink and downlink center frequencies are $f_{\text{UL}} = 2.5$ GHz and $f_{\text{DL}} = 2.62$ GHz. In each frequency band, the channel bandwidth is $W = 8$ MHz, divided into $N_C = 160$ OFDM subcarriers. The large-scale fading parameters and the path directions are kept constant over the uplink-downlink frequency gap. On the other hand, the small-scale

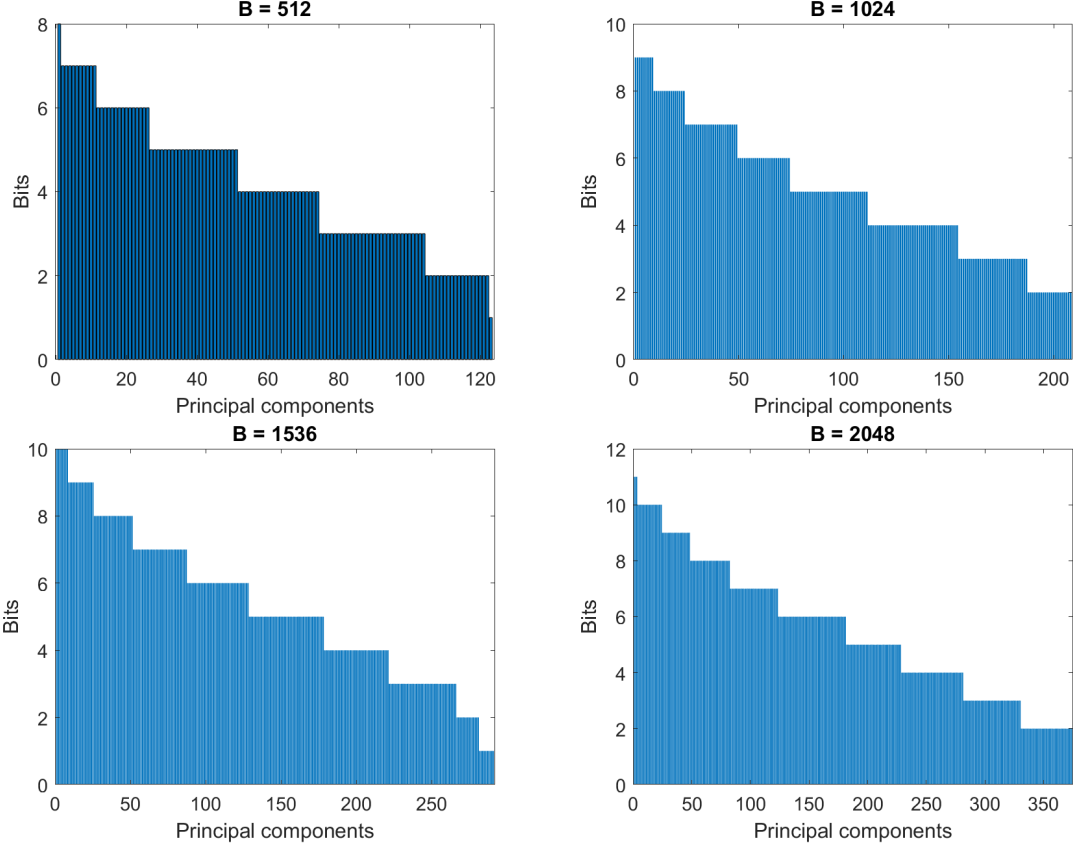


Fig. 3. Bit allocation to the principal components for four different values of B .

fading effects depend on the path phase-shifts, in turn dependent on the frequency. Thus, they are in practice uncorrelated over the frequency gap in rich multipath environments.

The channels resulting from the simulations contain the path loss, the large-scale fading, and small-scale fading effects. Thus, in order to work with scaled channels, we normalize the dataset according to

$$\mathbf{H}_{UL} \leftarrow L_{UL}^{-1} \mathbf{H}_{UL}, \mathbf{H}_{DL} \leftarrow L_{DL}^{-1} \mathbf{H}_{DL}, \quad (19)$$

where the scalars L_{UL}^{-1} and L_{DL}^{-1} contain the path loss and the large-scale fading effects. In total, $N = N_{\text{train}} + N_{\text{test}}$ users are randomly dropped in the cell and, for each user, the pair of channels $\mathbf{H}_{UL}, \mathbf{H}_{DL}$ is generated. Firstly, the *offline learning* stage is carried out considering N_{train} noisy uplink channel matrices. Secondly, the performance is tested on N_{test} downlink channel matrices, corresponding to the users not considered during the training phase. We assume that only noisy versions of the channel matrices are available both in the *offline learning* and *online development* stages, with $SNR_{UL} = 10$ dB and $SNR_{DL} = 10$ dB. The ground truth channels

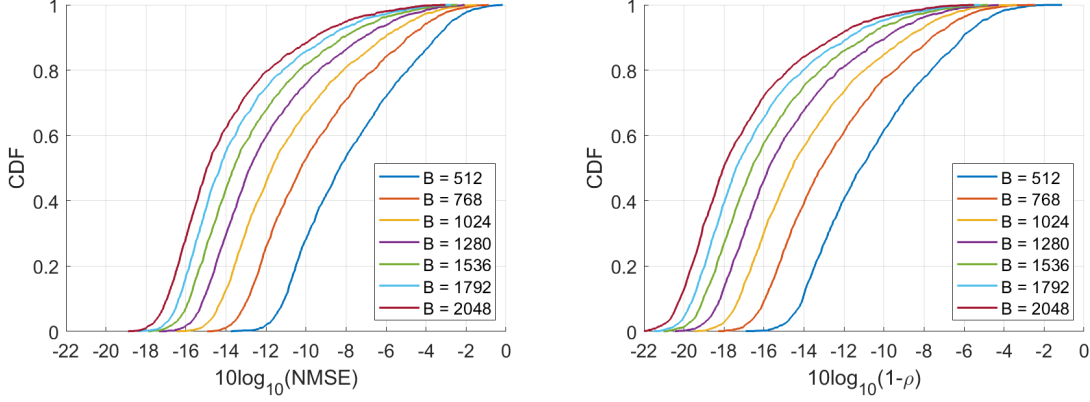


Fig. 4. NMSE (left) and cosine similarity (right) CDFs for different values of B .

\mathbf{H}_{DL} are only used to evaluate the reconstruction performance. Furthermore, we set $N_{\text{train}} = 5000$ and $N_{\text{test}} = 2000$.

B. Performance Evaluation

We now assess the performance of our PCA-based CSI feedback strategy. Experimentally, we noticed that the two modifications proposed in Section IV do not impact visibly the performance if $\eta \approx 16$ or less. Thus, the performance reported here refers to our proposed CSI feedback strategy including the two modifications with $\eta = 16$, unless otherwise specified. First of all, we inspect how the feedback bits are allocated to the principal components. In Fig. 3, we report a graphical representation of the vector \mathbf{b} resulting from Algorithm 1 applied to four different values of B . As expected, we observe that the number of considered principal components N_P and the number of bits assigned to the first principal component b_1 increase as B increases.

In Fig. 4, the NMSE and the cosine similarity ρ between the reconstructed and the true downlink channel matrices are reported. These cumulative distribution functions (CDFs), calculated over the whole test set, show that the reconstruction quality increases with B , and that, more importantly, no performance upper bound is present. In fact, B could be potentially increased until all the principal components are considered to embed the CSI. In this extreme case, approximately perfect channel reconstruction could be achieved. This property cannot be found in DL strategies recently proposed for CSI feedback. In these strategies, the reconstruction quality is always bounded by the latent space dimensionality, which is fixed regardless of the value of B .

Finally, we report the performance of multi-user precoding carried out with the reconstructed downlink channel matrices. More precisely, we use the reconstructed downlink channels to serve $K = 8$ UEs through zero-forcing beamforming with water-filling power allocation. Zero-forcing beamforming is applied independently to each subcarrier and the resulting sum rate is averaged over the N_C subcarriers. The water-filling power allocation is designed assuming that the reconstructed downlink channel is the perfect channel. Thus, the multi-user interference is not captured in the water-filling solution. In order to obtain reliable results, Monte Carlo simulations are run by randomly selecting, in each simulation, $K = 8$ downlink channels among the N_{test} available in the test set. Fig. 5 reports the average sum rate obtained by compressing the CSI with four different feedback lengths B . Here, our CSI feedback strategy, namely “PCA”, is compared with two baseline strategies based on DL architectures. “AE128”, “AE256”, “AE512”, and “AE1024” are the convolutional autoencoder proposed in [18], where the number of neurons in the middle layer is set to 128, 256, 512, and 1024, respectively. In addition, “CsiNet128”, “CsiNet256”, “CsiNet512”, and “CsiNet1024” are the CsiNet architecture proposed in [19], with the codeword size set to 128, 256, 512, and 1024, respectively.

For the two baseline strategies, the feedback bits are allocated uniformly to all the latent space dimensions, and the quantization levels are determined with k -means clustering. Denoting with N_L the latent space dimensionality, we have that $\frac{B}{N_L}$ bits are allocated to each dimension, with $N_L \in \{128, 256, 512, 1024\}$ in our comparison. Furthermore, to find the optimal quantization levels, we firstly compress the whole training set onto the latent space. Then, we independently apply one-dimensional k -means clustering on each latent space dimension. Preliminary experiments confirmed that $N_{\text{train}} = 5000$ training samples are not enough to well-train the “AE” and “CsiNet” architectures. With this amount of training data, these DL architectures are not able to learn an expressive representation of the channels in the latent space. For this reason, in Fig. 5, we report the performance of well-trained “AE” and “CsiNet” architectures, i.e., trained with 40000 training samples.

Among the two considered DL architectures, “AE” outperforms “CsiNet” for every considered B , as already highlighted in [18]. Furthermore, for the DL architectures, we notice that there is not a unique latent space dimensionality N_L that is optimal for every feedback length B . This result supports our intuition that N_L should be designed according to the number of bits B . Since we consider such an adaptive design, our strategy “PCA” performs approximately as the best autoencoder “AE” in every B considered. Thus, PCA can be successfully applied to

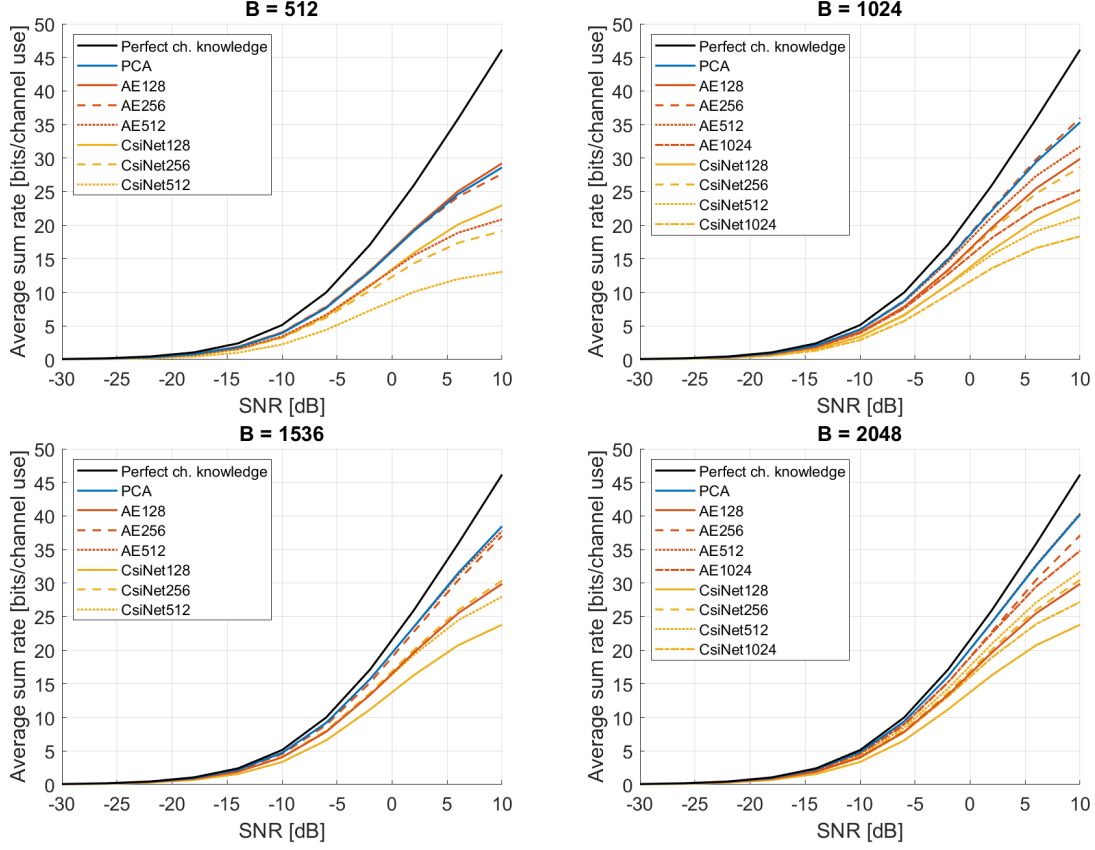


Fig. 5. Average sum rate with zero-forcing beamforming for four different values of B . “PCA” has been trained with 2000 samples, “AE” and “CsiNet” have been trained with 40000 samples.

compress the channel matrix with a significantly reduced training set.

To analyze the effect of the parameter η on the performance, we plot the average sum rate versus the feedback length B , by fixing the SNR experienced by each of the K user to 10 dB. In Fig. 6, the performance of our strategy is compared with the two considered baseline DL architectures, each with four different N_L . We notice that the performance of each DL architecture saturates as B increases due to the fixed latent space dimensionality. Thus, each N_L turns out to be optimal only for some specific values of B . More precisely, “AE128” is the best autoencoder when $B = 512$, “AE256” is preferred when $B \in \{768, 1024, 1280\}$, while “AE512” is the autoencoder achieving the highest average sum rate when $B \in \{1536, 1792, 2048\}$. The four “CsiNet” achieve a lower average sum rate than their respective “AE” architectures, as expected from [18]. Conversely, the performance of our PCA-based strategy with $\eta = 16$ is comparable with the one of the best autoencoder “AE” for each value of B . Furthermore, we can notice that the performance deterioration caused by increasing η is minimal.

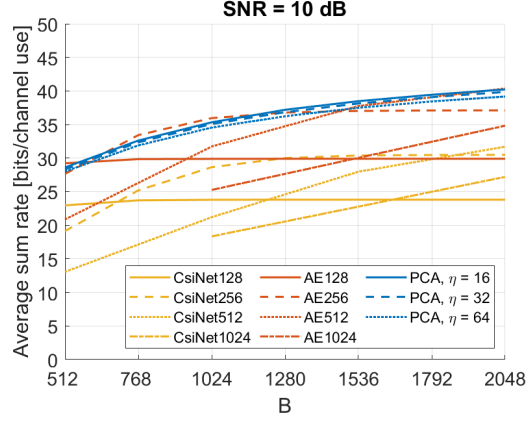


Fig. 6. Average sum rate with zero-forcing beamforming vs feedback length B , with $\text{SNR} = 10$ dB at each UE. “PCA” has been trained with 2000 samples, “AE” and “CsiNet” have been trained with 40000 samples.

C. Offloading Impact

We now analyze the impact of the two modifications proposed in Section IV on the overhead caused by parameter offloading. The effect of the first modification can be analyzed by comparing (13) with (14). When computing N_O^{model} , the number of offloaded parameters due to μ_{train} can be neglected, since in practice $N_P \gg 1$. Thus, we have that the first modification decreases the number of offloaded model parameters of approximately $\frac{2}{3}\eta$ times. In our numerical scenario, $B = 2048$ yields $N_P = 374$. Hence, without the first modification, we have $N_O^{\text{model}} = 7.68 \times 10^6$ according to (13). Conversely, when the first modification is applied with $\eta = 16$, N_O^{model} is reduced to 0.739×10^6 according to (14).

Considering the offloaded k -means clustering parameters, the effect of the second modification is given by comparing (15) with (16). Also to quantify the effect of the second modification, we refer to the case in which the maximum feedback length allowed is $B = 2048$, yielding $N_P = 374$ and $b_1 = 11$ in our numerical scenario. Without the second modification, we have $N_O^{k\text{-means}} = 243 \times 10^3$ according to (15). Conversely, when the second modification is applied, $N_O^{k\text{-means}}$ is reduced to 10.6×10^3 according to (16).

When both modifications are applied, we notice that $N_O^{\text{model}} \gg N_O^{k\text{-means}}$. Thus, now we compare our PCA-based CSI feedback strategy with the two baseline DL-based strategies in terms of offloaded model parameters, neglecting the offloaded k -means clustering parameters. This comparison is carried out in Fig. 7, where N_O^{model} is reported for our strategy when both modifications are considered, with $\eta \in \{16, 32, 64\}$. For the two considered DL architectures, an

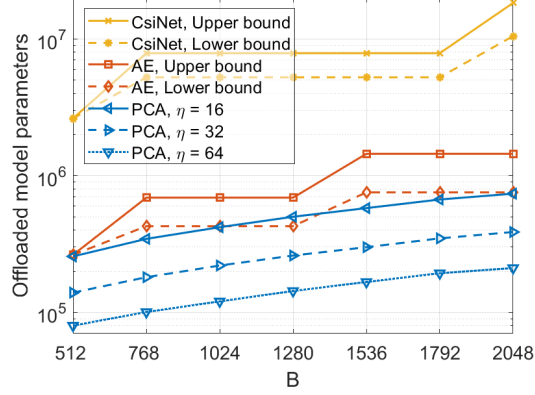


Fig. 7. Number of offloaded model parameters vs feedback length B . “PCA” has been trained with 2000 samples, “AE” and “CsiNet” have been trained with 40000 samples.

upper bound and a lower bound on the number of offloaded model parameters are reported. The upper bound represents the case in which we offload all the necessary encoders to generate a feedback of length less or equal than B . These encoders can be retrieved from Fig. 6, considering only the most performing ones for feedback lengths less or equal than B . In our numerical scenario, only the encoder of “AE128” is offloaded when $B = 512$; the encoders of “AE128” and “AE256” are offloaded when $B \in \{768, 1024, 1280\}$, and the encoders of “AE128”, “AE256”, and “AE512” are offloaded when $B \in \{1536, 1792, 2048\}$. With the same reasoning, only the encoder of “CsiNet128” is offloaded when $B = 512$; the encoders of “CsiNet128” and “CsiNet256” are offloaded when $B \in \{768, 1024, 1280, 1536, 1792\}$, and the encoders of “CsiNet128”, “CsiNet256”, and “CsiNet512” are offloaded when $B = 2048$. Thus, the upper bound is given by summing the parameters of the offloaded encoders for each B . The lower bound represents the case in which we apply the parallel multiple-rate framework proposed in [26]. In this framework, among the necessary encoders, only the encoder with the largest latent space dimensionality is offloaded. The other encoders are obtained at the UE by just considering a reduced number of latent space dimensions from this encoder. Note that this framework inevitably causes a slight degradation in the channel reconstruction performance, as stated in [26]. However, in this study we do not assess such a performance degradation.

Fig. 7 shows that our PCA-based strategy is convenient also in terms of offloading overhead compared with the two DL-based strategies, not only in terms of training samples required. When $\eta = 16$, our strategy and the “AE” strategy used with the framework proposed in [26]

TABLE I
PERFORMANCE COMPARISON WITH FEEDBACK LENGTH $B = 2048$.

	Average sum rate [bits/channel use]	Number of offloaded model parameters	Number of training samples
PCA, $\eta = 16$	40.2	0.739×10^6	5×10^3
PCA, $\eta = 32$	39.9	0.387×10^6	5×10^3
PCA, $\eta = 64$	39.2	0.211×10^6	5×10^3
AE	40.4	1.45×10^6	40×10^3
CsiNet	31.7	18.4×10^6	40×10^3

cause similar offloading overhead. However, thanks to the adaptive parameter η , in our strategy it is possible to significantly reduce this overhead by only slightly affecting the reconstruction performance, as shown in Fig. 6.

Finally, in Tab I we summarize the comparison between our PCA-based strategy and the two considered DL-based strategies, for a feedback length $B = 2048$. Here, the offloaded parameter number for the deep architectures are computed without considering the framework in [26], since it would cause a non-negligible performance degradation. Compared with “AE”, our strategy using $\eta = 16$ halves the offloading overhead and reduces the number of training samples by eight times. If $\eta = 64$ is considered, the offloading overhead is reduced by 6.87 times, at the cost of a 2.97% average sum rate loss. Compared with “CsiNet”, our strategy improves the average sum rate by 26.8% (resp. 23.7%), and reduces the offloading overhead by 24.9 (resp. 82.2) times, when $\eta = 16$ (resp. $\eta = 64$).

VI. CONCLUSION

In this study, we propose a novel strategy to design the CSI feedback in FDD massive MIMO systems. This strategy allows to design the feedback with variable length, while reducing the number of parameter offloaded from the BS to the UE. Firstly, the channel is compressed using PCA, with a latent space dimensionality adapted to the number of available feedback bits. Then, the feedback bits are allocated to the principal components by minimizing a properly defined NMSE distortion. Finally, the quantization levels are determined with k -means clustering. In addition, we allow an adaptive number of offloaded model parameters, which can be adjusted to trade offloading overhead and CSI reconstruction quality. Such an adaptive offloading overhead has been never considered in previous literature employing DL approaches.

Through simulations, we compare our strategy with state-of-the-art DL architectures proposed for the same scope. Numerical results show that our strategy performs better or approximately equal, to DL architectures well-trained on larger datasets, in terms of sum rate obtained with multi-user precoding. The offloading overhead can be significantly reduced in our strategy, with approximately no impact on the CSI reconstruction. At the same time, PCA is characterized by a lightweight training phase, requiring a reduced number of training samples. This lightweight training phase enables, in practical developments, more frequent trainings. In this way, the compression strategy could be better maintained updated, as the environment evolves in time. Compared with CsiNet, our strategy using $\eta = 16$ improves the average sum rate by 26.8%, reduces the offloading overhead by 24.9 times, and requires eight times fewer training parameters.

APPENDIX

A. Proof of Proposition 1

Since the bit allocation $\mathbf{b}' = [b'_1, \dots, b'_{N_A N_C}]$ contains one more bit than $\mathbf{b} = [b_1, \dots, b_{N_A N_C}]$, there is always a principal component m such that $b'_m = b_m + C$, with $C \geq 1$. Thus, to prove Proposition 1, we need to prove that the bit allocation $[b_1, \dots, b_m + 1, \dots, b_{N_A N_C}]$ is better than any other allocation of $B + 1$ bits $[b'_1, \dots, b_m + C, \dots, b'_{N_A N_C}]$. This is equivalent to saying that the distortion caused by $[b_1, \dots, b_m + 1, \dots, b_{N_A N_C}]$ is less than the distortion caused by $[b'_1, \dots, b_m + C, \dots, b'_{N_A N_C}]$, that is

$$\begin{aligned} d_1(b_1) + \dots + d_m(b_m + 1) + \dots + d_{N_A N_C}(b_{N_A N_C}) \\ < d_1(b'_1) + \dots + d_m(b_m + C) + \dots + d_{N_A N_C}(b'_{N_A N_C}) \end{aligned} \quad (20)$$

For convenience, we rewrite (20) as

$$\begin{aligned} [d_1(b_1) + \dots + d_m(b_m) + \dots + d_{N_A N_C}(b_{N_A N_C})] + [d_m(b_m + 1) - d_m(b_m)] \\ < [d_1(b'_1) + \dots + d_m(b_m + C - 1) + \dots + d_{N_A N_C}(b'_{N_A N_C})] + [d_m(b_m + C) - d_m(b_m + C - 1)], \end{aligned} \quad (21)$$

where two additive terms are highlighted in both sides of the inequality. Thus, (21) can be proved by independently verifying the following two inequalities

$$\begin{aligned} d_1(b_1) + \dots + d_m(b_m) + \dots + d_{N_A N_C}(b_{N_A N_C}) \\ < d_1(b'_1) + \dots + d_m(b_m + C - 1) + \dots + d_{N_A N_C}(b'_{N_A N_C}) \end{aligned} \quad (22)$$

$$d_m(b_m + 1) - d_m(b_m) \leq d_m(b_m + C) - d_m(b_m + C - 1). \quad (23)$$

Firstly, (22) holds since $\mathbf{b} = [b_1, \dots, b_{N_A N_C}]$ is the optimal bit allocation of B bits. Thus, any other allocation of B bits $[b'_1, \dots, b_m + C - 1, \dots, b'_{N_A N_C}]$ causes an higher distortion. Secondly, to prove (23), we need to resort to an explicit expression of the MSE distortion as a function of the quantization bit number. Since a close form expression of such a distortion in the case of k -means clustering is not available, we consider the distortion-rate function, which provides a lower bound on the MSE distortion [43]. According to information theory, the distortion-rate function of a CSCG random variable $X_n \sim \mathcal{CN}(0, \sigma_n^2)$ quantized with b_n bits is given by $d_n(b_n) = \sigma_n^2 2^{-b_n}$ [43]. Thus, assuming that on the n -th principal component the training set is distributed as $\mathcal{CN}(0, \sigma_n^2)$, (23) can be rewritten as

$$\sigma_m^2 2^{-(b_m+1)} - \sigma_m^2 2^{-b_m} \leq \sigma_m^2 2^{-(b_m+C)} - \sigma_m^2 2^{-(b_m+C-1)} \quad (24)$$

$$\sigma_m^2 2^{-b_m} (2^{-1} - 1) \leq \sigma_m^2 2^{-(b_m+C-1)} (2^{-1} - 1) \quad (25)$$

$$2^{-b_m} \geq 2^{-(b_m+C-1)}, \quad (26)$$

which is verified since $C \geq 1$.

B. Proof of Proposition 2

To prove Proposition 2, we prove that the optimal b_n cannot be greater than b_{n-1} since the bit allocation $b_{n-1} = C + \Delta C$, $b_n = C$ is always better than $b_{n-1} = C$, $b_n = C + \Delta C$, where $C \in \mathbb{N}$, $\Delta C \in \mathbb{N}^*$. This means that

$$d_{n-1}(C + \Delta C) + d_n(C) < d_{n-1}(C) + d_n(C + \Delta C), \quad (27)$$

since the best bit allocation to the two principal components $n-1$ and n is the one that minimizes the distortion $d_{n-1} + d_n$. As in Appendix A, we write the distortion caused by quantizing the n -th principal component with b_n bits as $d_n(b_n) = \sigma_n^2 2^{-b_n}$. Thus, (27) can be rewritten as

$$\sigma_{n-1}^2 2^{-(C+\Delta C)} + \sigma_n^2 2^{-C} < \sigma_{n-1}^2 2^{-C} + \sigma_n^2 2^{-(C+\Delta C)} \quad (28)$$

$$\sigma_n^2 2^{-C} - \sigma_n^2 2^{-(C+\Delta C)} < \sigma_{n-1}^2 2^{-C} - \sigma_{n-1}^2 2^{-(C+\Delta C)} \quad (29)$$

$$\sigma_n^2 2^{-C} (1 - 2^{-\Delta C}) < \sigma_{n-1}^2 2^{-C} (1 - 2^{-\Delta C}), \quad (30)$$

which is verified since the principal components are ordered, i.e., $\sigma_n^2 < \sigma_{n-1}^2$.

C. Proof of Proposition 3

The goal of k -means clustering is to group the N dataset points into k clusters, and to assign a unique quantization level to each cluster. This is done by minimizing the sum of the square distances between each data point and the quantization level assigned to its cluster [38]. Let us denote with \mathbf{x}_n the n -th point in the dataset \mathbf{X} . The k -means clustering process can be formalized by introducing the binary indicator $r_{ni} \in \{0, 1\}$ such that $r_{ni} = 1$ if \mathbf{x}_n is assigned to the i -th cluster, and $r_{ni} = 0$ otherwise. In this way, the optimal clustering indicators $\{r_{ni}\}^*$ and quantization levels $\{\mathbf{q}_i\}^*$ are given by

$$\{r_{ni}\}^*, \{\mathbf{q}_i\}^* = \min_{\{r_{ni}\}, \{\mathbf{q}_i\}} \sum_{n=1}^N \sum_{i=1}^k r_{ni} \|\mathbf{x}_n - \mathbf{q}_i\|^2. \quad (31)$$

Now, let us consider the scaled dataset $\mathbf{Y} = c\mathbf{X}$, in which \mathbf{y}_n is the n -th point. In this case, the optimal clustering indicators $\{r'_{ni}\}^*$ and quantization levels $\{\mathbf{q}'_i\}^*$ are

$$\{r'_{ni}\}^*, \{\mathbf{q}'_i\}^* = \min_{\{r'_{ni}\}, \{\mathbf{q}'_i\}} \sum_{n=1}^N \sum_{i=1}^k r'_{ni} \|\mathbf{y}_n - \mathbf{q}'_i\|^2 \quad (32)$$

$$= \min_{\{r'_{ni}\}, \{\mathbf{q}'_i\}} \sum_{n=1}^N \sum_{i=1}^k r'_{ni} \|c\mathbf{x}_n - \mathbf{q}'_i\|^2 \quad (33)$$

$$= \min_{\{r'_{ni}\}, \{\mathbf{q}'_i\}} \sum_{n=1}^N \sum_{i=1}^k r'_{ni} \left\| \mathbf{x}_n - \frac{1}{c} \mathbf{q}'_i \right\|^2, \quad (34)$$

where the objective function in (33) has been multiplied by the scalar c^{-2} to obtain (34). Noting that the minimization problem in (34) is equal to (31), it holds $\{r'_{ni}\}^* = \{r_{ni}\}^*$ and $\frac{1}{c}\{\mathbf{q}'_i\}^* = \{\mathbf{q}_i\}^*$. Thus, we verified that $\{\mathbf{q}'_i\}^* = c\{\mathbf{q}_i\}^*$.

REFERENCES

- [1] B. Clerckx and C. Oestges, *MIMO wireless networks: Channels, techniques and standards for multi-antenna, multi-user and multi-cell systems*. Academic Press, 2013.
- [2] D. J. Love, R. W. Heath, V. K. N. Lau, D. Gesbert, B. D. Rao, and M. Andrews, "An overview of limited feedback in wireless communication systems," *IEEE Journal on Selected Areas in Communications*, vol. 26, no. 8, pp. 1341–1365, 2008.
- [3] J. Choi, D. J. Love, and P. Bidigare, "Downlink training techniques for FDD massive MIMO systems: Open-loop and closed-loop training with memory," *IEEE Journal of Selected Topics in Signal Processing*, vol. 8, no. 5, pp. 802–814, 2014.
- [4] X. Rao and V. K. N. Lau, "Distributed compressive CSIT estimation and feedback for FDD multi-user massive MIMO systems," *IEEE Transactions on Signal Processing*, vol. 62, no. 12, pp. 3261–3271, 2014.

- [5] Z. Gao, L. Dai, Z. Wang, and S. Chen, "Spatially common sparsity based adaptive channel estimation and feedback for FDD massive MIMO," *IEEE Transactions on Signal Processing*, vol. 63, no. 23, pp. 6169–6183, 2015.
- [6] A. Adhikary, J. Nam, J.-Y. Ahn, and G. Caire, "Joint spatial division and multiplexing-the large-scale array regime," *IEEE Transactions on Information Theory*, vol. 59, no. 10, pp. 6441–6463, 2013.
- [7] Y. Xu, G. Yue, and S. Mao, "User grouping for massive MIMO in FDD systems: New design methods and analysis," *IEEE Access*, vol. 2, pp. 947–959, 2014.
- [8] M. Dai, B. Clerckx, D. Gesbert, and G. Caire, "A rate splitting strategy for massive MIMO with imperfect CSIT," *IEEE Transactions on Wireless Communications*, vol. 15, no. 7, pp. 4611–4624, 2016.
- [9] M. Alrabeiah and A. Alkhateeb, "Deep learning for TDD and FDD massive MIMO: Mapping channels in space and frequency," in *2019 53rd Asilomar Conference on Signals, Systems, and Computers*, 2019, pp. 1465–1470.
- [10] M. Arnold, S. Dörner, S. Cammerer, S. Yan, J. Hoydis, and S. t. Brink, "Enabling FDD massive MIMO through deep learning-based channel prediction," *arXiv preprint arXiv:1901.03664*, 2019.
- [11] Y. Yang, F. Gao, G. Y. Li, and M. Jian, "Deep learning-based downlink channel prediction for FDD massive MIMO system," *IEEE Communications Letters*, vol. 23, no. 11, pp. 1994–1998, 2019.
- [12] P. Dong, H. Zhang, G. Y. Li, N. NaderiAlizadeh, and I. S. Gaspar, "Deep CNN for wideband mmwave massive MIMO channel estimation using frequency correlation," in *ICASSP 2019 - 2019 IEEE International Conference on Acoustics, Speech and Signal Processing (ICASSP)*, 2019, pp. 4529–4533.
- [13] Y. Han, M. Li, S. Jin, C.-K. Wen, and X. Ma, "Deep learning-based FDD non-stationary massive MIMO downlink channel reconstruction," *IEEE Journal on Selected Areas in Communications*, vol. 38, no. 9, pp. 1980–1993, 2020.
- [14] M. S. Safari, V. Pourahmadi, and S. Sodagari, "Deep UL2DL: Data-driven channel knowledge transfer from uplink to downlink," *IEEE Open Journal of Vehicular Technology*, vol. 1, pp. 29–44, 2020.
- [15] J. Wang, Y. Ding, S. Bian, Y. Peng, M. Liu, and G. Gui, "UL-CSI data driven deep learning for predicting DL-CSI in cellular FDD systems," *IEEE Access*, vol. 7, pp. 96 105–96 112, 2019.
- [16] V. Rizzello, I. Brayek, M. Joham, and W. Utschick, "Learning the channel state information across the frequency division gap in wireless communications," in *WSA 2020; 24th International ITG Workshop on Smart Antennas*, 2020, pp. 1–6.
- [17] J. Guo, C.-K. Wen, and S. Jin, "CANet: Uplink-aided downlink channel acquisition in FDD massive MIMO using deep learning," *IEEE Transactions on Communications*, pp. 1–1, 2021.
- [18] V. Rizzello and W. Utschick, "Learning the CSI denoising and feedback without supervision," in *2021 IEEE 22nd International Workshop on Signal Processing Advances in Wireless Communications (SPAWC)*, 2021, pp. 16–20.
- [19] C.-K. Wen, W.-T. Shih, and S. Jin, "Deep learning for massive MIMO CSI feedback," *IEEE Wireless Communications Letters*, vol. 7, no. 5, pp. 748–751, 2018.
- [20] Z. Liu, L. Zhang, and Z. Ding, "Exploiting bi-directional channel reciprocity in deep learning for low rate massive MIMO CSI feedback," *IEEE Wireless Communications Letters*, vol. 8, no. 3, pp. 889–892, 2019.
- [21] —, "An efficient deep learning framework for low rate massive MIMO CSI reporting," *IEEE Transactions on Communications*, vol. 68, no. 8, pp. 4761–4772, 2020.
- [22] Z. Cao, W.-T. Shih, J. Guo, C.-K. Wen, and S. Jin, "Lightweight convolutional neural networks for CSI feedback in massive MIMO," *IEEE Communications Letters*, vol. 25, no. 8, pp. 2624–2628, 2021.
- [23] Y. Sun, W. Xu, L. Liang, N. Wang, G. Y. Li, and X. You, "A lightweight deep network for efficient CSI feedback in massive MIMO systems," *IEEE Wireless Communications Letters*, vol. 10, no. 8, pp. 1840–1844, 2021.
- [24] S. Jo and J. So, "Adaptive lightweight CNN-based CSI feedback for massive MIMO systems," *IEEE Wireless Communications Letters*, vol. 10, no. 12, pp. 2776–2780, 2021.

- [25] T. Wang, C.-K. Wen, S. Jin, and G. Y. Li, "Deep learning-based CSI feedback approach for time-varying massive MIMO channels," *IEEE Wireless Communications Letters*, vol. 8, no. 2, pp. 416–419, 2019.
- [26] J. Guo, C.-K. Wen, S. Jin, and G. Y. Li, "Convolutional neural network-based multiple-rate compressive sensing for massive MIMO CSI feedback: Design, simulation, and analysis," *IEEE Transactions on Wireless Communications*, vol. 19, no. 4, pp. 2827–2840, 2020.
- [27] Z. Lu, X. Zhang, H. He, J. Wang, and J. Song, "Binarized aggregated network with quantization: Flexible deep learning deployment for CSI feedback in massive MIMO system," *IEEE Transactions on Wireless Communications*, pp. 1–1, 2022.
- [28] J. Guo, L. Wang, F. Li, and J. Xue, "CSI feedback with model-driven deep learning of massive MIMO systems," *IEEE Communications Letters*, pp. 1–1, 2021.
- [29] M. Soltani, V. Pourahmadi, A. Mirzaei, and H. Sheikhzadeh, "Deep learning-based channel estimation," *IEEE Communications Letters*, vol. 23, no. 4, pp. 652–655, 2019.
- [30] W. Utschick, V. Rizzello, M. Joham, Z. Ma, and L. Piazzi, "Learning the CSI recovery in FDD systems," *IEEE Transactions on Wireless Communications*, pp. 1–1, 2022.
- [31] P. Liang, J. Fan, W. Shen, Z. Qin, and G. Y. Li, "Deep learning and compressive sensing-based CSI feedback in FDD massive MIMO systems," *IEEE Transactions on Vehicular Technology*, vol. 69, no. 8, pp. 9217–9222, 2020.
- [32] N. Turan, M. Koller, S. Bazzi, W. Xu, and W. Utschick, "Unsupervised learning of adaptive codebooks for deep feedback encoding in FDD systems," in *2021 55th Asilomar Conference on Signals, Systems, and Computers*, 2021, pp. 1464–1469.
- [33] M. Chen, J. Guo, C.-K. Wen, S. Jin, G. Y. Li, and A. Yang, "Deep learning-based implicit CSI feedback in massive mimo," *IEEE Transactions on Communications*, vol. 70, no. 2, pp. 935–950, 2022.
- [34] F. Sohrabi, K. M. Attiah, and W. Yu, "Deep learning for distributed channel feedback and multiuser precoding in FDD massive MIMO," *IEEE Transactions on Wireless Communications*, vol. 20, no. 7, pp. 4044–4057, 2021.
- [35] J. Guo, C.-K. Wen, and S. Jin, "Deep learning-based CSI feedback for beamforming in single- and multi-cell massive MIMO systems," *IEEE Journal on Selected Areas in Communications*, vol. 39, no. 7, pp. 1872–1884, 2021.
- [36] V. Rizzello, N. Turan, M. Joham, and W. Utschick, "Two-sample tests for validating the UL-DL conjecture in FDD systems," in *2021 17th International Symposium on Wireless Communication Systems (ISWCS)*, 2021, pp. 1–6.
- [37] J. Zeng, J. Sun, G. Gui, B. Adebisi, T. Ohtsuki, H. Gacanin, and H. Sari, "Downlink CSI feedback algorithm with deep transfer learning for FDD massive MIMO systems," *IEEE Transactions on Cognitive Communications and Networking*, vol. 7, no. 4, pp. 1253–1265, 2021.
- [38] C. M. Bishop, *Pattern Recognition and Machine Learning*. Springer Verlag, Aug. 2006.
- [39] A. Ge, T. Zhang, Z. Hu, and Z. Zeng, "Principal component analysis based limited feedback scheme for massive MIMO systems," in *2015 IEEE 26th Annual International Symposium on Personal, Indoor, and Mobile Radio Communications (PIMRC)*, 2015, pp. 326–331.
- [40] J. Joung, E. Kurniawan, and S. Sun, "Channel correlation modeling and its application to massive MIMO channel feedback reduction," *IEEE Transactions on Vehicular Technology*, vol. 66, no. 5, pp. 3787–3797, 2016.
- [41] D. Tse and P. Viswanath, *Fundamentals of wireless communication*. Cambridge university press, 2005.
- [42] S. Jaeckel, L. Raschkowski, K. Börner, and L. Thiele, "QuaDRiGa: A 3-D multi-cell channel model with time evolution for enabling virtual field trials," *IEEE Transactions on Antennas and Propagation*, vol. 62, no. 6, pp. 3242–3256, 2014.
- [43] T. M. Cover, *Elements of information theory*. John Wiley & Sons, 1999.